INVESTIGATION OF THE ABILITY OF RELAP5/MOD3 TO MODEL NATURAL CIRCULATION OF HIGH PRESSURE SF_6 IN THE WESTINGHOUSE 1/7 SCALE PWR EXPERIMENTAL FACILITY

by

STEFAN VINCENT CHMIELEWSKI

SUBMITTED TO THE DEPARTMENT OF
NUCLEAR ENGINEERING
IN PARTIAL FULFILLMENT OF THE REQUIREMENTS
FOR THE DEGREES OF

BACHELOR OF SCIENCE

and

MASTER OF SCIENCE

at the

MASSACHUSETTS INSTITUTE OF TECHNOLOGY

February, 1992

Signature of Author Signature redacted
Department of Nuclear Engineering
January 17, 1992

Certified by Signature redacted
Peter Griffith
Professor of Mechanical Engineering
Thesis Supervisor

Certified by Signature redacted
Neil E. Todreas
Professor of Nuclear Engineering
Thesis Reader

Accepted by Signature redacted
Allan F. Henry
Chairman, Department Graduate Committee
Department of Nuclear Engineering

INVESTIGATION OF THE ABILITY OF RELAP5/MOD3 TO MODEL NATURAL CIRCULATION OF HIGH PRESSURE SF_6 IN THE WESTINGHOUSE 1/7 SCALE PWR EXPERIMENTAL FACILITY

by

STEFAN VINCENT CHMIELEWSKI

Submitted to the Department of Nuclear Engineering
on January 17, 1992 in partial fulfillment of the
requirements for the Degrees of Bachelor of Science and
Master of Science in Nuclear Engineering

ABSTRACT

The RELAP5/MOD3 capability to predict high pressure SF_6 natural circulation test results from a 1/7 scale pressurized water reactor (PWR) model was examined. Assessment calculations using RELAP5/MOD3 were performed to determine how well the code could duplicate the hot leg test results. The RELAP5/MOD3 hot leg model was configured to simulate a sloped countercurrent flow in the hot legs of the model, with the slope of the countercurrent interface being one of the variables in the problem. Certain geometric constants were varied in the RELAP5/MOD3 model until reasonable agreement with experimental results was achieved. These constants were then applied to a model of the hot leg for a full-size PWR to calculate transient conditions which would induce natural circulation. This application demonstrated that the hot leg model adjustments derived by matching the Westinghouse data had minimal effect upon the duration and sequence of the predicted natural circulation transient failure events.

Peter Griffith
Professor of Mechanical Engineering
Thesis Advisor

and

Neil E. Todreas
Professor of Nuclear Engineering
Thesis Reader

ACKNOWLEDGEMENTS

My heartfelt thanks to all who helped in this effort, particularly those at EG&G Idaho, Inc. who provided input, support, and attitude adjustment at the appropriate times. This list of names includes Larry, Duane, Paul, Chuck, Doug, Ken, Sandy S., Sandy H., and Ed. Thanks also to Professor Griffith, for providing guidance, and to Jean, for just being there.

CONTENTS

LIST OF FIGURES

LIST OF TABLES

INVESTIGATION OF THE ABILITY OF RELAP5/MOD3 TO MODEL NATURAL CIRCULATION OF HIGH PRESSURE SF_6 IN THE WESTINGHOUSE 1/7 SCALE PWR EXPERIMENTAL FACILITY

1.0 INTRODUCTION

1.1 BACKGROUND

During severe accident scenarios involving loss of decay heat removal, the reactor primary coolant boils off, which leads to fuel heat-up and failure. It is generally believed that the steam formed during boil-off of the primary coolant inventory naturally circulates through the primary system in an established flow pattern. This natural convection serves to remove decay heat from the core and deposit it in structures above the core and in the hot legs, which slows the core heat-up phase of the transient, leading to slower core damage progression.

Of particular concern is a transient in which the coolant boils off and the core melts through the lower head while the system is at an elevated pressure. Such a sequence would result in molten corium being forcibly ejected, due to the high pressures within the vessel, into containment, leading to direct containment heating (DCH). This is a worst-case scenario for the type of transient discussed above. However, the natural circulation within the reactor pressure vessel (RPV) convects energy from the core to structures within the vessel and in the hot legs. This energy transfer has the potential to heat up and result in the failure of structures in other parts of the primary system before the core melts through the lower head and into containment. If the pressure boundary in the primary system fails before the core melt-through of the lower head, the primary system would depressurize. Ejection of corium into containment at low pressure is a much less catastrophic event for containment.

1.2 NATURAL CIRCULATION

During a postulated severe accident with loss of decay heat removal, it is believed that a buoyancy driven flow pattern arises in the reactor coolant system (RCS) due to steaming in the core. For the case where the cold leg loop seals are blocked by water, two separate flow patterns can be identified: in-vessel circulation and hot leg countercurrent flow. Figure 1 shows these natural circulation flow patterns both in and out of the RPV. The net effect of such a natural circulation flow is to transfer heat generated in the core to other parts of the primary system, such as to the upper plenum internals, the hot legs, and the steam generator tubing, which leads to these structures heating up.

1.2.1 In-Vessel Natural Circulation

In-vessel natural circulation begins at the onset of core heatup. The radial power distribution in the core is peaked in the center, which causes the fluid in the center part to be hotter and less dense than at the periphery of the core. Thus, fluid rises from the center of the core into the upper plenum region of the RPV, while the denser, cooler vapor in the outer sections of the core tends to flow back toward the center of the core, replacing fluid that rises into the upper plenum. As the fluid rises, it is cooled by metal in the upper plenum, and it is eventually turned aside as it reaches the top of the upper plenum. At this point, the fluid flows radially outward to the core barrel, where, because of the density change induced in the fluid by the cooling process, it begins to flow downward into the outer fuel elements of the core. There the fluid reenters the core through the peripheral fuel assemblies. As core uncovery progresses and the liquid level drops in the RPV, this natural circulation flow pattern extends further down into the core.

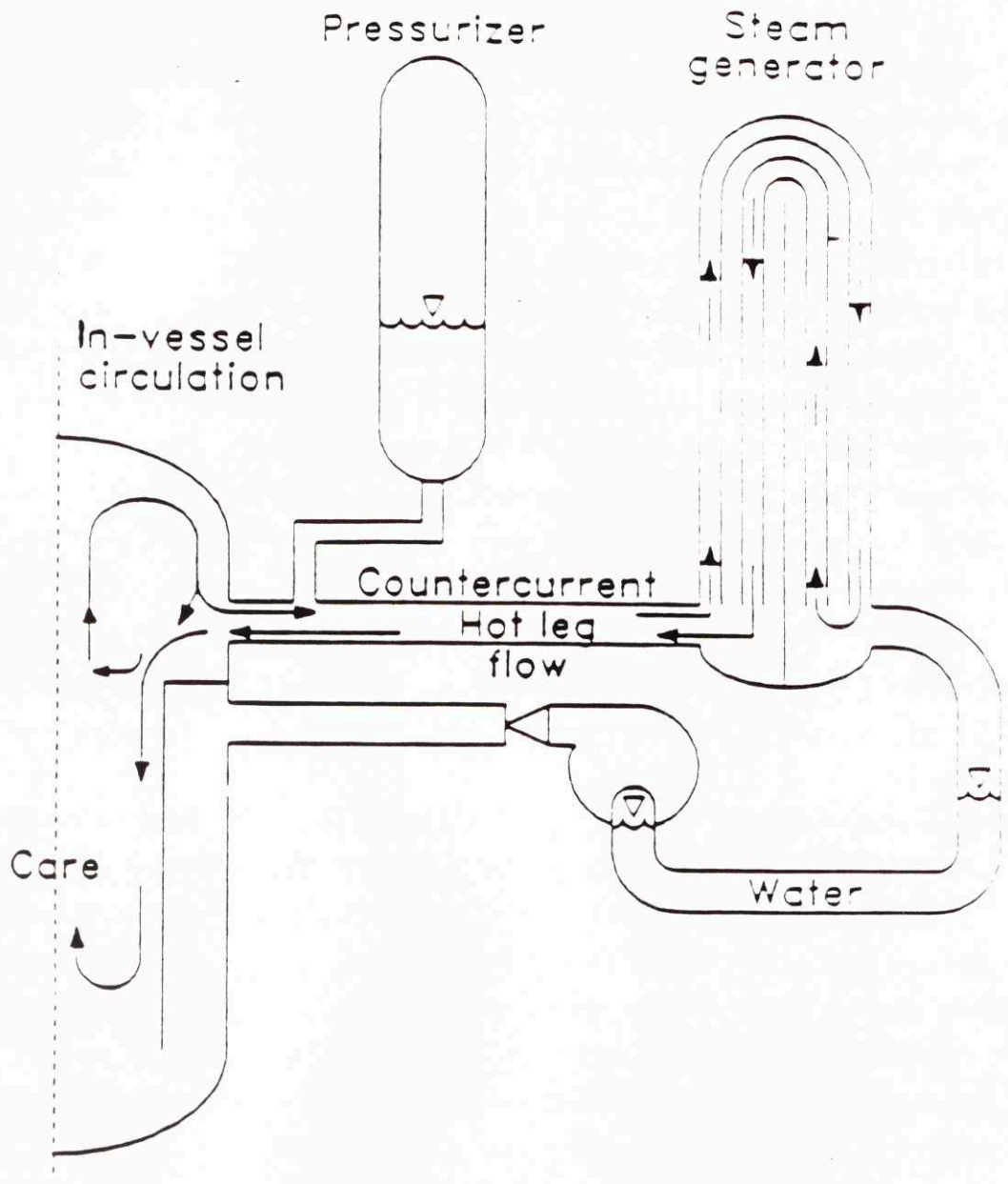

Figure 1. Natural Circulation flow pattern both in-vessel and ex-vessel during some severe accidents. Flow rises from the core into the upper plenum, where it splits to flow into the hot legs and back down into the core. Hot leg countercurrent flow arises, as does steam generator tube flow.

1.2.2 Hot Leg Countercurrent Flow

Hot fluid in the upper plenum may also flow through the hot legs and reach the steam generator. It is believed that the hot vapor flows into the top of the hot leg, causing the cooler vapor already present in the hot leg to flow back along the bottom of the pipe to the RPV, where it adds to the flow downward along the core barrel. The hot vapor is cooled during its transit through the hot leg by the piping walls and by the walls of the steam generator inlet plenum. When the hot vapor enters the inlet plenum, some of the vapor enters some of the steam generator tubes and, due to buoyancy differences, flows through these steam generator tubes to the outlet plenum of the steam generator. An effect of this is to displace vapor from the remaining tubes and from the steam generator outlet plenum into the steam generator inlet plenum, where it mixes with and reduces the temperature of the vapor in the inlet plenum, which then flows back along the bottom of the hot leg to the RPV.

Since the cold leg loop seals would be blocked by subcooled liquid, flow would be blocked from returning to the RPV via the cold legs. Also, the vapor would be further cooled by the walls of the outlet plenum and cold leg and by the liquid-vapor interface in the cold leg. In addition, the tubes of the steam generator would act as a heat sink. Cooler vapor would then be induced to flow back through other steam generator tubing to the steam generator inlet plenum, where the mixing pattern mentioned above would occur, causing cooler fluid to flow back to the RPV.

1.3 BASIS FOR STUDY

As mentioned before, the net effect of such a natural circulation flow is to transfer heat generated in the core to other parts of the primary system, such as to the upper plenum internals, the hot legs, and the steam generator tubing, which leads to these structures heating up and possibly failing due to heat-induced creep rupture. Furthermore,

during a high pressure boil-off transient, the power-operated relief valve (PORV) cycles, drawing superheated vapor into the pressurizer surge line, and making the surge line an additional heat sink, as well as a possible candidate location for failure due to heat-induced creep rupture.

If reactor coolant system piping ruptures before molten material breaks through the lower head of the RPV, the vessel pressure is reduced and the outcome of the transient is changed dramatically. As mentioned above, a high-pressure blowdown of molten core material would result in direct containment heating. However, a low pressure environment within the RPV could result in more severe steam explosions as a result of the core material relocating to the lower head where liquid is still present. In addition, depending upon where the failure of the pressure boundary occurs due to creep rupture, the containment barrier may be bypassed via steam generator tube failure. Thus, natural circulation may drastically alter the timing and outcome of some transient events.

The flow patterns and some of the possible outcomes described above were experimentally emulated by a set of experiments performed at the Westinghouse Electric Corporation's Research and Development Center.[1] There, a 1/7 scale model of a Westinghouse four loop PWR was designed and constructed, and tests were performed. Reference 1 gives a description of the model. Initially, two sets of experiments were performed, one using low pressure water, and the other using SF_6 at low pressure. However, Westinghouse determined that high pressure SF_6 more adequately modeled high pressure steam, thus providing better similitude between the experiment and the actual full-scale case.[2] A battery of high pressure tests using SF_6 as the working fluid were then performed. Reference 2 documents the results of these high pressure tests.

It is desirable to have a calculational basis for empirically observed natural circulation effects. RELAP5/MOD3 provides a way to computationally model such effects. RELAP5/MOD3 is a one-dimensional thermal-hydraulics code used in severe accident analyses of nuclear

systems. The code uses best-estimate integral calculations to model the thermal-hydraulic and core damage response. It is therefore able to explicitly determine the effect of natural circulation flows of the type described above on system damage progression.

2.0 PROCEDURES

2.1 AREA OF STUDY

The areas of interest in this task were defined early in the study. Three "milestones" were identified, which follow.

1. A RELAP5/MOD3 hot leg model was constructed to simulate the Westinghouse experimental data and to allow comparisons between the results obtained using RELAP5/MOD3 to selected Westinghouse experimental data in the hot legs and steam generators. The purpose of this was to establish the values of geometric constants which best reproduce the Westinghouse high pressure SF_6 results when using a one-dimensional code like RELAP5/MOD3. The geometric constants of particular interest were f_w, the wall friction factor, considered to be an average value over the hydraulic flow diameter; f_i, the interface friction factor, which will be incorporated into the wall friction factor; F_m, the mixing fraction in the steam generator inlet plenum; and $\blacksquare_i$, the slope of the hot/cold countercurrent interface in the hot leg.

2. Once the model was constructed, runs were performed using RELAP5/MOD3 to calculate the "typical" conditions for SF_6 in the model. During these runs, the values of the geometric constants were varied in order to obtain values for which the Westinghouse experimental results were reproduced by the code. When the Westinghouse results were matched, the values of these constants were "frozen".

3. After the proper values for the geometric constants in the hot leg were found such that the RELAP5/MOD3 calculations matched the Westinghouse experimental results, the hot leg computational model was used for a full-size

PWR. This full-size model was altered by incorporating the values of the geometric constants derived in task number two. That is, the full-size PWR hot leg model had a sloped countercurrent flow interface, a steam generator inlet plenum divided into a hot, a mixing, and a cold volume, and an effective friction factor which accounted for a countercurrent flow interface. Then, a transient analysis was performed to examine where and when the pressure boundary first failed as a result of creep rupture. The failure times and locations were compared to those obtained in similar analyses which used other geometries in the hot leg. Locations which are candidates for failure due to creep rupture as a result of natural circulation include the pressurizer surge line, the hot leg where it joins the RPV, and the steam generator tubing just above the level of the tubesheet.

2.2 PROCEDURES

In accordance to the above list of tasks, a model of the Westinghouse 1/7 scale PWR experimental apparatus was constructed.[3] The model can be broken down into two subsections: the RPV and the hot legs.

2.2.1 RPV Computational Model

The experimental model fluid flow paths in the reactor pressure vessel of the Westinghouse experimental apparatus and the associated internal structures were simulated very closely and accurately. (This was verified by an independent assessor.) The description of the reactor internals was taken from Reference 1. Both the upper plenum and the core structures were broken up into a number of flow cells, allowing for natural circulation behavior to occur.

Many considerations went into building an input deck to model the

Westinghouse 1/7 scale PWR experimental apparatus. Initially, the RPV and its internals had to be modeled by reasonable small flow components in order to allow for multi-directional flow, especially in the upper plenum. The division of the upper plenum into smaller, multi-directional flow components also needed a logical basis in geometry. Thus, the upper plenum was divided according to natural lines of reference which could be pictured from a side view of the apparatus. In particular, the area level with the hot leg entrance (nozzle), both top and bottom, marked two levels of division. Furthermore, since flow both entered and exited the hot leg nozzle, there was another division made even with the midpoint of the nozzle.

A nodalization diagram of the RPV and its internals for the RELAP5/MOD3 model is given as Figure 2. The core has three channels, each corresponding to a differing power level radially across the core. These three channels allow multi-directional flow between core cells. There are eight core cells axially along each core channel, corresponding to subdivisions which occur in the experimental apparatus. Also, all communication paths from the upper plenum to the upper head are accounted for, as is the metal within the system.

Within the upper plenum of the RELAP5/MOD3 model, the flow cells are divided up according to the geometry of the Westinghouse experimental apparatus. The upper plenum in the apparatus contains guide tube assemblies, support columns, and communications tubes which connect the upper plenum to the upper head. The support columns exist only in the top of the upper plenum, while the communication tubes extend almost to the upper core plate. Figure 3 is a schematic display of the relative positions of the upper plenum internals in the experimental model. Figure 3 also identifies the heights at which the upper plenum was divided into vertical flow volumes for insertion into the RELAP5/MOD3 model. For example, the lowest flow cell in the upper plenum extends only as high as the bottom of the hot leg nozzle. Also, the level corresponding to the hot leg pipe itself is divided in half, with a flow cell level occurring at the lower half of the hot leg, and

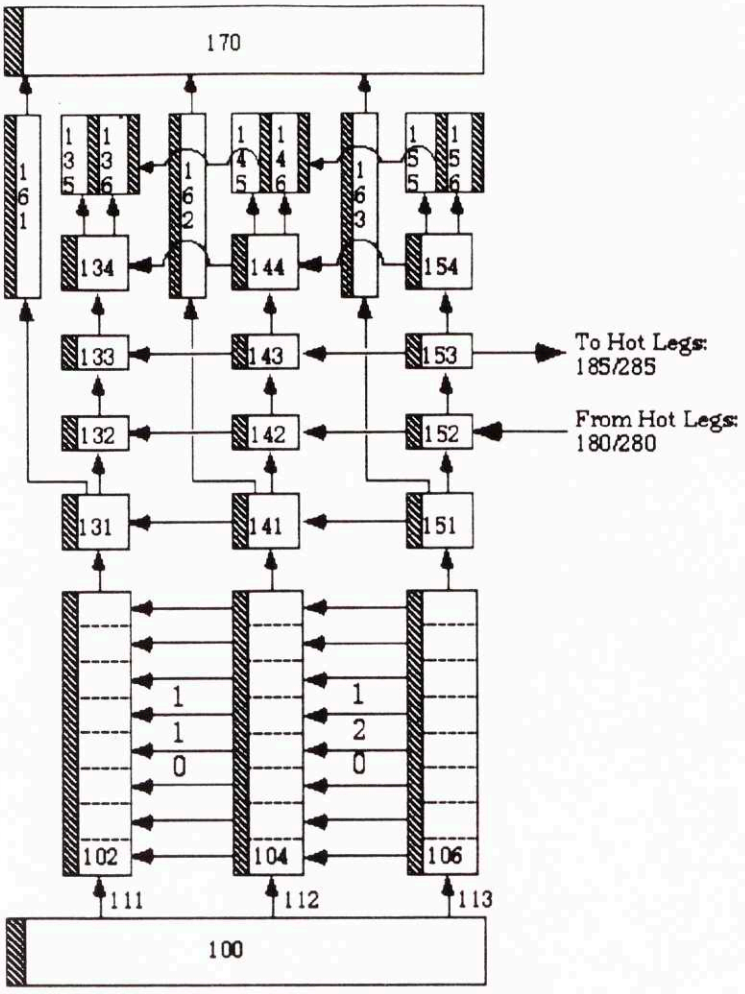

Figure 2. The nodalization diagram of the RPV is shown. Note the three channel core and the multi-directional flow volumes in the upper plenum. These multi-directional flow volumes enable natural circulation to occur throughout the RPV. Shaded areas represent metal structures. The arrows indicate the positive flow direction, not necessarily the actual direction of flow.

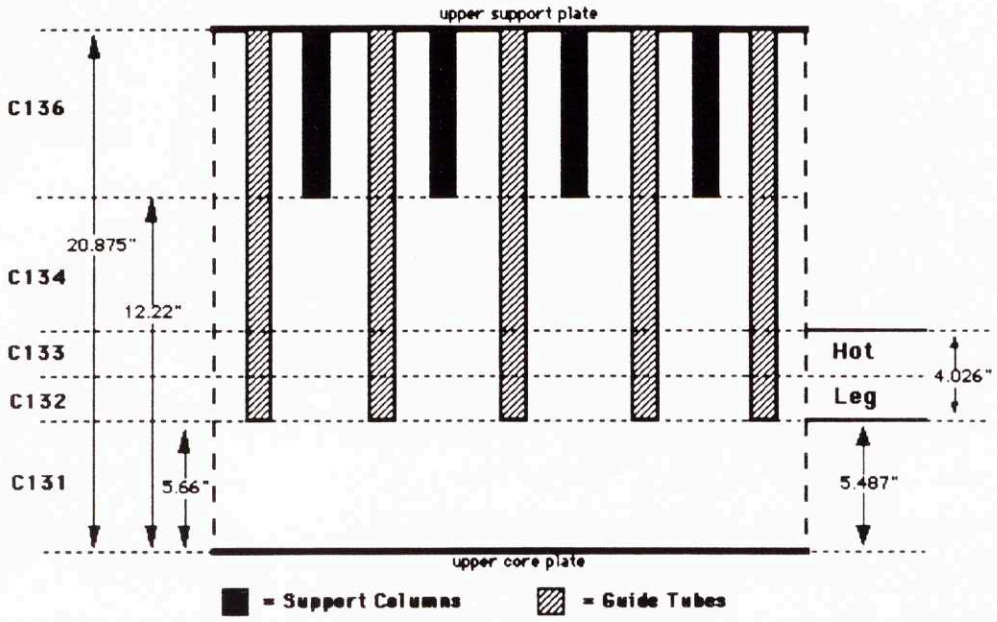

Figure 3. Schematic view of upper plenum geometry in the Westinghouse experimental apparatus, leading to considerations in devising the nodalization of the upper plenum for the RELAP5/MOD3 model. Note the divisions at heights level with the endpoints of certain structures in the upper plenum, such as the hot leg pipe level, the support column level, etc.

another flow cell level occurring at the upper half of the hot leg. Thus, considerations for geometry and flow in multiple directions are made.

2.2.2 Hot Leg Computational Model

Since RELAP5/MOD3 is a one-dimensional code, the only way to model two-directional flow in one pipe such as that which occurs in a countercurrent hot leg flow is to model the single pipe as two pipes with counterdirectional flow paths. The model of the split pipe then follows as closely as possible the flow geometry of the actual pipe being modeled. Thus, since natural circulation was anticipated to divide flow areas in the hot leg into counterdirectional flows, a split hot leg was designed. Previous split hot leg designs divided the total flow area of the hot leg pipe equally between the two countercurrent flows.[3] However, Westinghouse observed during experimentation that under steady-state conditions, 72% of the flow area in the hot leg where the hot leg connects to the RPV was involved in hot fluid flow toward the steam generator inlet plenum. As this stream flowed down the hot leg, the flow area gradually decreased until, at the point where the hot fluid stream entered the steam generator inlet plenum, only 28% of the flow area of the hot leg was utilized by the hot flow stream. Likewise, the return countercurrent cold fluid stream initially occupied 72% of the hot leg flow area as it exited the steam generator inlet plenum, but by the time it reached the hot leg nozzle at the RPV, the cold stream occupied only 28% of the total hot leg flow area. Thus, the counterflowing hot and cold streams were observed to interact along a sloped interface within the hot leg.

For the purposes of this analysis, then, a split hot leg was constructed. The split hot leg consisted of two pipes, one for each flow direction, both of which started with a large fraction of the total flow area in the hot leg but decreased in flow area gradually until the end of the flow stream path was reached. A nodalization diagram of the hot leg is given as Figure 4. However, Figure 4 does not accurately

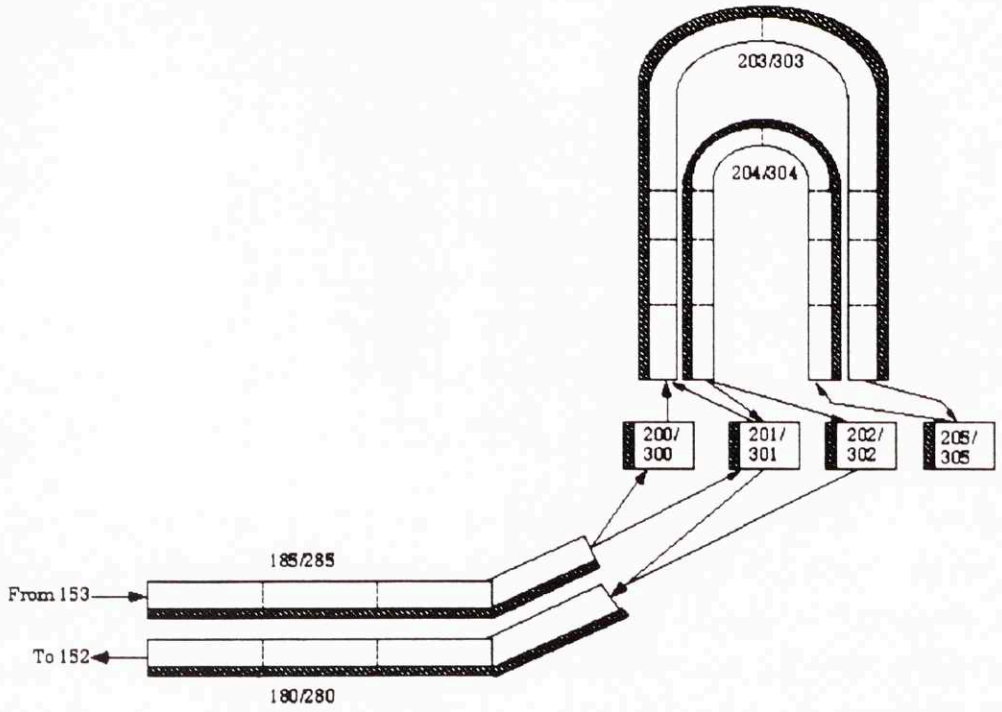

Figure 4. The nodalization diagram of the hot leg is shown. This is a split, countercurrent flow hot leg model. However, the split hot leg shown does not represent accurately the sloped portion of the hot leg. There is no pressurizer modeled because the Westinghouse apparatus did not have one. Again, shaded areas represent metal structures.

portray the flow area reduction as a function of flow length for the two flow directions in the hot leg. Appendix A contains the methodology for the construction of the split hot leg, including that methodology used to initialize the geometrical values for the hot leg.

2.2.3 Code Modifications

Once the RELAP5/MOD3 model of the Westinghouse experimental apparatus was constructed, attention turned to matching the hot leg tests of the Westinghouse experiments which used high pressure SF_6. However, since RELAP5/MOD3 did not initially contain thermodynamic data for SF_6, some code modifications were in order.

RELAP5/MOD3 contains an option which allows all of a particular volume to be filled with a noncondensible gas. Using this option, one could initialize all volumes in the main flow system as being filled with the gas of choice. Once this was determined, an effort was made to insert relevant properties of SF_6 into the code so that the code could treat the gas as a noncondensible. However, this step assumes that SF_6 behaves as a perfect gas, which is incorrect. This is a good assumption at low pressures, as shown by a graph of compressibility factors in Reference 2. At higher pressures, though, SF_6 tends to compress more at low temperatures than at high.

At first glance, the assumption that SF_6 behaves as a perfect gas seems incorrect. However, the temperature regime in which the experiments were performed was sufficiently high that at steady-state conditions, the performance of SF_6 deviated from the performance of a perfect gas by only about 10%. This value initially seemed significant. Thus, simple benchmarking tests, such as adding heat to a single flow volume and comparing the code-calculated temperature rise to expected values, were performed with the code. At low temperatures, large (>10%) temperature variations were found, with the code over-predicting the temperature increase. This overprediction was traced to the methodology by which the code initializes the mass of fluid in any particular

volume. Since SF_6 would normally compress at high pressures, more fluid mass would actually be present in a volume than the code would initialize, so the thermal inertia of any code-calculated volume would initially be too low and the calculated temperature increase would be too rapid. However, once the volume reached steady-state conditions at higher temperatures, the rate of temperature increase leveled off so that predicted values and code-calculated values of temperature converged.

At the point where high temperature steady-state conditions are reached, the rate of fluid expansion becomes very small and the thermal inertia of any volume becomes constant. At these high temperatures, the difference between the amount of fluid calculated by the code to be in the volume versus the actual amount of fluid that is in a volume is very small. Since the Westinghouse experimental apparatus had a relief valve attached which allowed for fluid expansion during heat-up to steady-state conditions, then the rate of expansion in the experimental apparatus would also level off, as would the thermal inertia of the system. Because only steady-state conditions were to be examined in this work, it was determined that a perfect gas approximation was acceptable.

Values for the molecular weight of SF_6, as well as for C_p and C_v, were thus inserted into the code.[6] Using the noncondensible option described above, the RELAP5 model of the Westinghouse 1/7 scale experimental facility was tested, and once all bugs were worked out or fixed, attempts began to match selected Westinghouse experimental results.

2.2.4 Experimental Matching

The Westinghouse reports contain results for a number of experiments performed using SF_6 as the working fluid under both steady-state and transient conditions. Of particular interest are the steady-state tests which emphasized the phenomena that occur in the hot leg

TABLE 1. STEAM GENERATOR STEADY-STATE GOVERNING PARAMETERS[a]

Test Number	SG-S1	SG-S2	SG-S3	SG-S4
SF_6 Pressure (psia)	300	400	300	400
Core Power (kW)	22	22	30	30

a. From Table 4-13, page 4-83, of Reference 2.

piping and in the steam generator itself. Four tests were performed by Westinghouse which fit these conditions. The governing parameters which were varied to make each test different are pressure and core power level. These parameters are given in Table 1.

As can be seen from Table 1, the difference between the steady-state steam generator tests was minimal. The tests which were chosen to model were tests numbered SG-S1 and SG-S2. Table 2 lists reported results for these two tests. These tests were chosen for a number of reasons. Most important among these reasons was the fact that earlier test number S-8 was performed at a similar power level. Unfortunately, the results of tests SG-S1 and SG-S2 did not report the amount of heat removal performed in the upper plenum and in the hot legs. But steady-state test S-8 did report this information, and the same percentage values for heat removal from test S-8 were used in order to match the two steam generator tests. Table 3 lists heat removal data from test S-8. Also, since both tests SG-S1 and SG-S2 were performed at the same power, it was a simple task to just change the operating pressure of the model. Ideally, it would have been desirable to use a test which operated at steady-state conditions, which focused on phenomena in the hot legs and steam generators, and which adequately documented all boundary conditions of the test. Unfortunately, such a test was not documented in the Westinghouse reports.

Initially, the steam generator inlet plenum was divided into three regions: a hot region, a mixing region, and a cold region. In earlier studies which examined natural circulation, 95% of the steam generator inlet plenum volume was in the mixing region. 65% of the remaining 5% of the volume was located in the cold region, while 35% of the remaining 5% was located in the hot region.[5] However, the Westinghouse experimental results reported that the mixing fraction in the steam generator inlet plenum was .87-.89, or 87-89%. Thus, in this RELAP5/MOD3 model, 89% of the steam generator inlet plenum volume was located in the mixing region. By selecting the larger value for the mixing volume, allowance is made for the maximum amount of mixing to

TABLE 2. REPORTED RESULTS OF TESTS SG-S1 AND SG-S2[a]

Test Number	SG-S1	SG-S2
SF_6 Pressure (psia)	300	400
Core Power (kW)	22	22
Number of Hot Tubes	75	62
Number of Cold Tubes	141	154
Hot Leg Mass Flow (lbm/s)	0.115	0.180
Mixing Fraction, F_m	0.87	0.89

a. From Table 4-13, page 4-83, of Reference 2.

TABLE 3. HEAT REMOVAL DATA FROM TEST S-8[a]

Heat Removed	(kW)	(%)
Upper Internals	9.10	47
Upper Plenum Wall	3.80	20
Right Steam Generator	3.35	17
Left Steam Generator	3.02	16
Total	19.27	
Core Heating	20.97	
% Heat Removed		91.89

a. Taken from Figure 4-19, page 4-25, of Reference 2. Test S-8 operated at 375 psia, 21.0 kW Core Heating.

occur in the steam generator inlet plenum.

The remaining 11% of the steam generator inlet plenum volume was split evenly between the hot and cold regions. The flow area to the hot legs and steam generator tubing was split in a similar fashion. As for the steam generator tubes themselves, previous analyses had initialized 35% of the total number of tubes as hot flow from the inlet plenum to the outlet plenum, and the remaining 65% of the tubes contained cooler flow from the outlet plenum to the inlet plenum.[4] As shown in Table 2, Westinghouse identified 34.7% of the tubes in test SG-S1 as being hot flow, while in test SG-S2, 28.7% of the tubes carried hot fluid. Because of flow velocity considerations, it was determined acceptable to initialize the percentage of steam generator tubes which carried hot fluid at 35%, with the remaining tubes carrying cooler fluid. By selecting the larger value, the flow velocity in the steam generator tubing is limited, preventing the code-calculated Reynolds number, and the associated other dimensionless constants, from altering the outcome of the calculation.

The other important parameters in the hot leg were the friction factors, f_i and f_w. Both of these values are calculated internally in RELAP5/MOD3 from user-input values of D_h, the hydraulic flow diameter, and ϵ, the surface roughness of the pipe. For f_i, it was assumed that the friction along the hot/cold interface would be similar to that for a very rough pipe (ϵ = 0.05). The rest of the pipe is considered to be commercial steel (ϵ = 0.00015). Then, to calculate f_w, a perimeter averaged value for the roughness is necessary (see Appendix A). The perimeter averaged value, then, is a function of the slope of the hot/cold interface, from which one determines the percentage of flow perimeter that is very rough.

Once all of the parameters of interest were set to an acceptable value, computational runs commenced. It was necessary, however, to first choose which flow values given in the Westinghouse experimental results were to be matched. The best thermodynamic values to match in

the hot legs were the mass flow rates of the gas, the temperature of the gas in each flow stream, and the density differences between the countercurrent flow streams. The Westinghouse results reported that the time to reach steady-state conditions was on the order of two hours, so most computer runs were initially run for 3600 seconds of problem time. After this period of time, plots of the comparison values mentioned above were examined and values calculated by the code were compared to values reported in the experimental results.

If comparison values did not match, the variable which was changed was the pressure loss coefficient in the hot legs. This K_{loss} value affected primarily the mass flow rates through the hot legs. The problem was then rerun until a steady-state condition was reached. This process was repeated until mass flow values for the hot leg flows were matched.

The next comparison value which was matched was the temperature of the flow streams. The temperature of the fluid entering the hot leg from the RPV was affected most by the amount of heat removed in the upper plenum by the upper internals. Thus, in order to match the temperature of the flow streams, it was planned to vary the amount of heat removed in the upper plenum slightly until matching conditions were obtained. Also, the returning cooler fluid along the bottom of the hot leg was affected most by the amount of cooling which occurred in the steam generator and in the steam generator outlet plenum. Values for the heat removal in these areas were also to be varied until matching conditions were obtained. However, it was discovered that after matching the mass flow rates in all parts of the hot leg, the temperatures of the fluid were very close to the experimentally determined values, and thus no heat removal changes were made.

The last comparison value, density difference between the hot and cold fluid streams in the hot leg, is governed solely by temperature at constant pressure and is related by the inverse of the temperature ratio. Since all of these tests were run at a constant pressure when at

steady-state conditions, once temperature data had been matched as described above, then density difference data had also been matched.

2.2.5 Full Scale Model

After tests SG-S1 and SG-S2 were matched using the comparison values mentioned above, then the values for the geometric constants involving the hot leg were applied to a full-size PWR RELAP5/MOD3 model. The model chosen was the Surry plant model, a Westinghouse 3-loop PWR. While the Westinghouse 1/7 scale experimental model represents a 4-loop system, the geometry of the hot legs for such a plant is little different from the hot leg geometry of a 3-loop system. Since the Surry model was readily available, it was the model chosen to be modified according to the results obtained in the matching of the Westinghouse experiments.

The transient model chosen for the Surry input deck was what is known as the TMLB′ sequence. This sequence represents a loss of both on-site and off-site electrical power, coupled with a loss of all decay heat removal. The sequence progresses to a high-pressure boil-off and core uncovery, which leads to the conditions of natural circulation flow. The Surry input deck was modified such that the hot leg flow areas for each direction of the countercurrent flows were made comparable to that used in the model of the Westinghouse experimental apparatus. Thus, 72% of the hot leg flow area at the point where the hot leg connects to the RPV was utilized by the hot stream flowing towards the steam generator inlet plenum, while 28% of the flow area at that location was utilized by the cooler stream flowing from the steam generator inlet plenum back to the RPV. Also, at the point where the hot leg connects to the steam generator inlet plenum, 72% of the flow area was taken by the cooler stream, while 28% of the flow area was taken by the hot stream.

In a similar fashion, the steam generator inlet plenum volume was divided according to $F_{\blacksquare} = 0.89$. Thus, 89% of the volume of the steam

generator inlet plenum was in the mixing component, while the remaining 11% of the volume was split evenly between the hot and cold components. The junction connection flow areas were divided according to the same value of $F_{\blacksquare}$. Additionally, 35% of the steam generator tubes was allocated to hot fluid flow from the inlet plenum to the outlet plenum, and the remaining 65% of the tubes was allocated to cooler fluid flow from the steam generator outlet plenum to the inlet plenum.

Once the modifications to the Surry TMLB' input deck were complete, the transient was run to failure. The failure times so obtained were then compared with failure times previously calculated with a normal split hot leg configuration. No significant differences in failure sequence or timing were observed.

3.0 RESULTS AND DISCUSSION

3.1 MODEL RUNS

Once all modeling considerations were taken into account, steady-state runs were performed to match the results generated in the Westinghouse 1/7 scale experiments. Table 4 lists important parameters of each test. This information originates in the Westinghouse experimental results.

Initially, test SG-S2 was run. Figure 5 shows a progression of restarts in order to converge upon the correct mass flow rate in the hot leg. Figure 6 shows calculated versus measured temperatures in the hot leg. This test was run for one hour of problem time (3600 seconds), after which, the time was reset to zero. Then, in 1000 second increments, the value of the pressure loss coefficient, k_{loss}, was varied to cause convergence with the experimental results. Table 5 compares experimental results with calculated results, along with associated error. It can be seen that RELAP5/MOD3 performed well once the model was set in an acceptable fashion.

The transition from test SG-S2 to test SG-S1 was minor, only involving changing the operating pressure. However, since at a lower pressure the thermal inertia is lower (due to lower mass per volume), the heat removal ratios needed to be changed before the proper temperature could be realized. Figure 7 shows the progression toward convergence of the mass flow in the hot legs. Figure 8 shows the calculated versus measured temperatures, while Table 6 compares the experimental results with the calculated results, along with associated error.

Errors were only calculated for deviations in mass flow and in the ΔT between the counterdirectional hot and cold streams in the hot leg. Calculating error based on absolute temperature differences would

TABLE 4. CONDITIONS TO MATCH IN THE HOT LEGS

Test	SG-S2	SG-S1
Pressure (psia)	400	300
mass flow (kg/s)	0.0816	0.0522
T_h (K)	388	397
T_c (K)	345	343

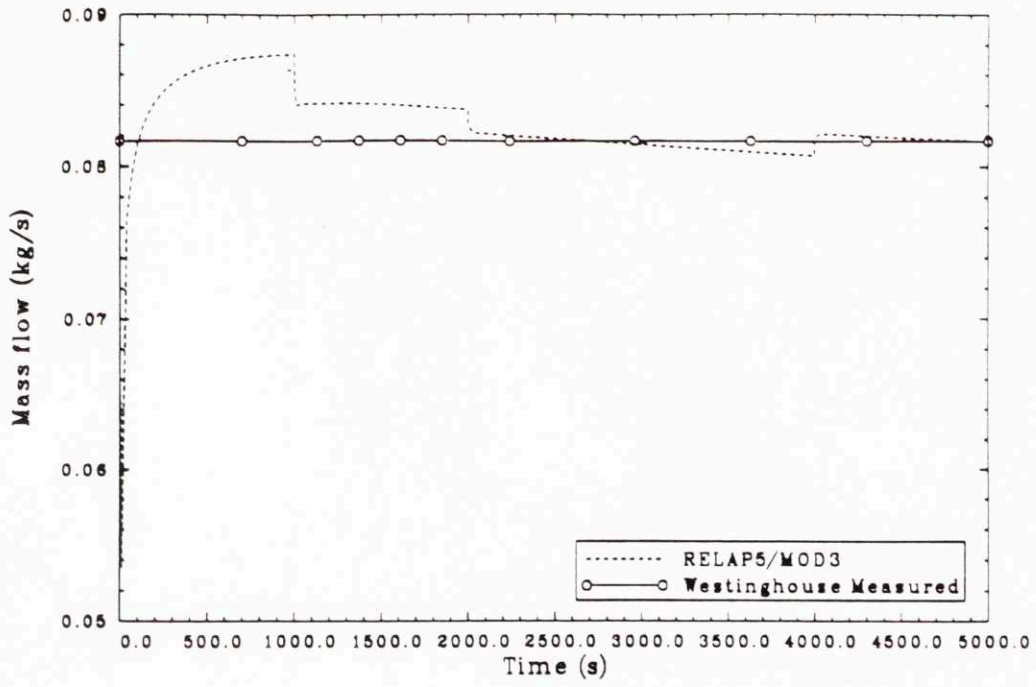

Figure 5. Mass flow rate (kg/s) vs. time (s) in the hot leg for test SG-S2. This problem was restarted every 1000 s with different k_{loss} values in order to effect convergence with experimentally measured results.

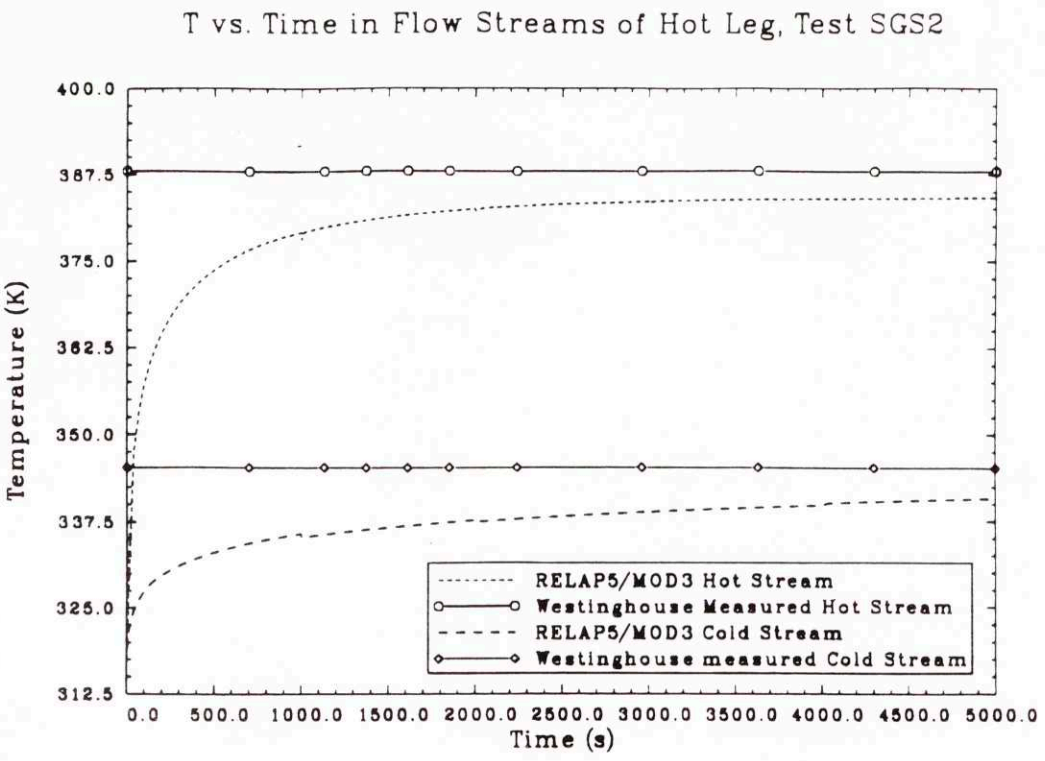

Figure 6. Temperature values, measured and calculated, for flow streams in the hot leg for test SG-S2. This problem was restarted every 1000 s with different k_{loss} values in order to effect convergence with experimental results.

TABLE 5. COMPARISON OF EXPERIMENTAL WITH COMPUTATIONAL TEST RESULTS FOR TEST SG-S2

	Experimental	Computational	Error(%)
Hot Leg:			
Mass Flow (kg/s)	0.08165	0.08161	0.049
Hot Stream, T_h (K)	387.95	384.211	
Cold Stream, T_c (K)	345.25	340.683	
Hot Leg ΔT (K)	42.7	43.5278	1.938
SG Inlet Plenum:			
Mixing Temp, T_m (K)	351.15	352.894	0.497
Hot Tube Temp, T_{ht} (K)	353.35	338.2856	
Cold Tube Temp, T_{ct} (K)	330.45	325.1672	

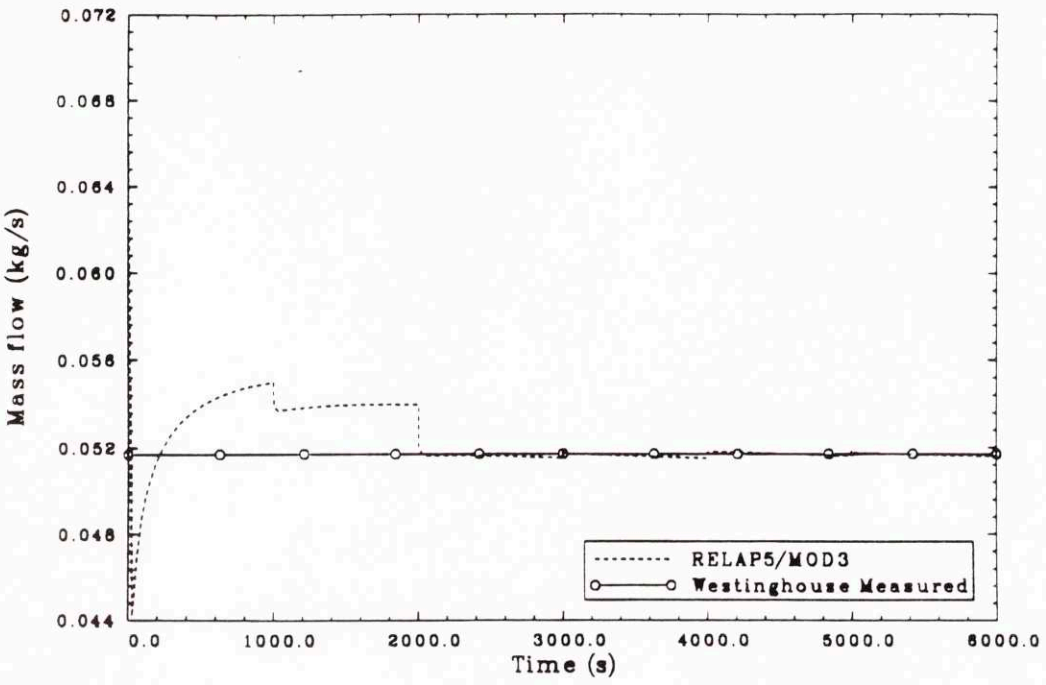

Figure 7. Calculated mass flow rate (kg/s) vs. time (s) in the hot leg for test SG-S1 as compared to Westinghouse experimental results.

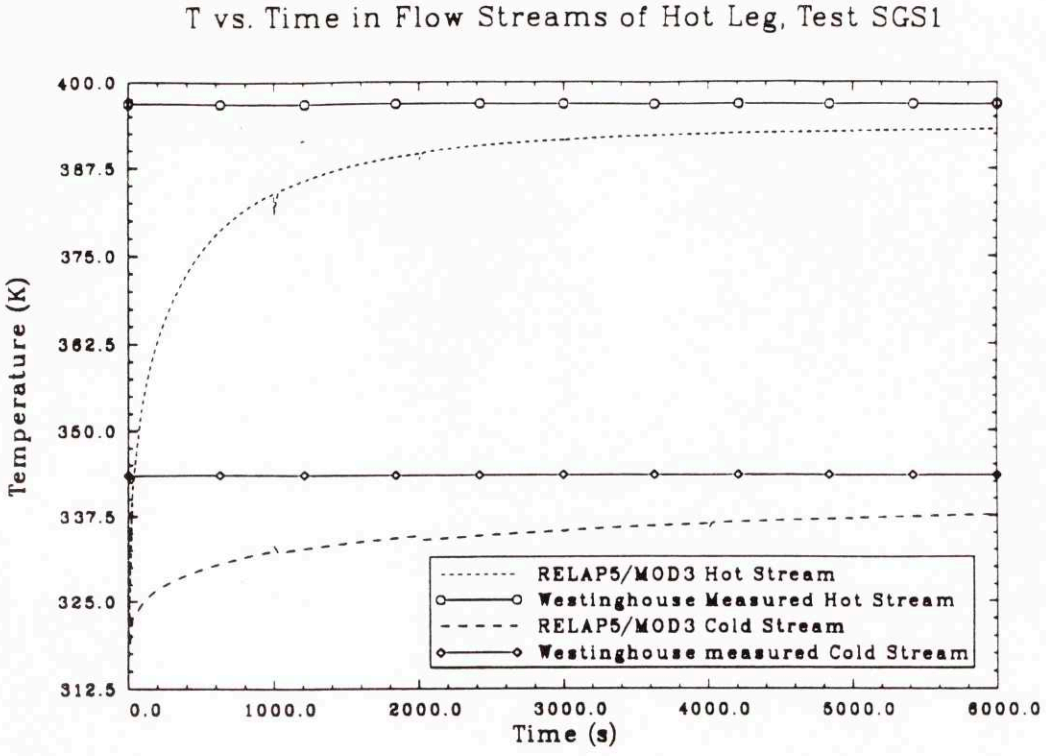

Figure 8. Calculated temperature (K) vs. time (s) for the two flow streams in the hot legs during test SG-S1 as compared to Westinghouse experimental results.

TABLE 6. COMPARISON OF EXPERIMENTAL WITH COMPUTATIONAL TEST RESULTS FOR TEST SG-S1

	Experimental	Computational	Error(%)
Hot Leg:			
Mass Flow (kg/s)	0.05216	0.05159	1.090
Hot Stream, T_h (K)	396.85	393.2111	
Cold Stream, T_c (K)	343.45	337.6722	
Hot Leg ΔT (K)	53.4	55.5389	4.005
SG Inlet Plenum:			
Mixing Temp, T_m (K)	350.05	353.965	1.118
Hot Tube Temp, T_{ht} (K)	352.85	338.349	
Cold Tube Temp, T_{ct} (K)	328.55	324.894	

distort the results by giving very small values. However, since the ΔT between the hot leg streams is on the order of 40 K, a two or three degree difference in ΔT would translate into higher, more realistic error estimates. Still, errors, in most cases, were less than two percent. Even the largest error, that of the ΔT of the hot leg counterdirectional streams in test SG-S1, was about four percent. And it is also clear from the tables that the temperature differences on an absolute scale between values measured in the Westinghouse experiments and values calculated by RELAP5/MOD3 are not significantly different.

3.2 SURRY PLANT MODEL

After the two Westinghouse tests were matched, the geometric constants identified were used in a full-size PWR model for the Surry plant. Like the model of the Westinghouse apparatus, the hot leg was split into a sloped countercurrent flow pattern, with 72% of flow area initially associated with the inlet of hot fluid and 28% of flow area associated with outflow of hot fluid. The same ratios also held for cold fluid flow. The steam generator inlet plenum was divided according to a mixing fraction, $F_{\blacksquare}$, of 0.89. The model was then run to failure for two cases.

In the first case, the friction of the countercurrent flow interface (hot/cold) was approximated to be that of a very rough pipe (f_i = 0.05). The surface roughness in the hot leg was then a flow perimeter averaged value. In the second case, the surface roughness was just that for commercially drawn steel (f_i = 1.5e-4). In this way, friction effects on the heat transfer to the walls of the hot leg pipe could be examined.

As a comparison point for this work, a concurrent analysis was performed. The other analysis used the unmodified version of the Surry RELAP5/MOD3 input deck. This unmodified input deck also contained a split hot leg for countercurrent flow modeling, but the split hot leg did not contain a sloped interface. In this way, data from the revised

TABLE 7. COMPARISON OF THE REVISED SPLIT HOT LEG SURRY TESTS TO A CONVENTIONAL SPLIT HOT LEG TEST

	Revised Split Hot Leg[a] (f_i = 0.05)[b]	(f_i = 1.5e-4)	Conventional Hot Leg
Time to Failure (s):			
Pressurizer Surge Line	14435.0	14475.0	14485.0
Hot Leg/RPV Junction (Avg)	15803.3	15795.0	15741.7
Lower Head Failure	17265.1	16660.0	16665.0
First Slump to Lower Head	16694.0	16282.4	16278.8

a. The revised split hot leg is the split hot leg with the sloped countercurrent flow modeled.

b. Entries under this heading correspond to those runs with the revised (sloped) split hot leg which takes into account increased friction due to a countercurrent flow interface.

split hot leg tests could be compared with data from a simple split hot leg, with all other factors being equal. Table 7 compares the results of this analysis to the results of the concurrent analysis.

In a full-size plant, one would expect the effects of natural circulation to prolong the transient. Heat would be convected away from the core and deposited faster in the upper internals and in the hot leg, heating up the metal. Thus, it is expected that the RCS pressure boundary integrity would be breached faster in a model which has an enhanced natural circulation geometry: that is, one that contains a sloped countercurrent flow interface. Additionally, because heat is being removed from the core faster in an enhanced situation, one would expect the lower head to fail due to fuel melt-through after a longer period of heat-up. While Table 7 demonstrates that this is the case, the failure times are not significantly different.

As a further comparison point, in the case where the friction factor is increased due to accounting for a countercurrent flow interface (f_i = 0.05), one would expect that the heat transfer coefficient from the fluid to the metal walls would be enhanced by a higher friction coefficient. A higher heat transfer rate would result, causing the metal in the hot legs to fail faster than in the case with no interface friction. Again, Table 7 confirms that this is true.

As can be seen from the results, the pressurizer surge line is the first part to fail in all of the tests. However, in the test where the hot leg friction factor is higher, the surge line fails earliest, but not by a significant amount of time. Once failure does occur, then blowdown ensues. The next location which fails is the junction where the hot leg connects to the RPV. All cases failed at this junction in about the same time.

That test which failed earliest demonstrated the latest lower head failure time, which again fits well with the theory that heat is removed from the core and deposited in the upper internals and in the piping of

the primary system. Here, the difference in failure times is about ten minutes, a slightly significant value. However, when one considers that the length of this transient from beginning to failure is on the order of 240 minutes, even ten minutes deviation is not appreciable.

For the case where the friction factor was the same as the value in the conventional test, it appears that the sloped configuration of the hot leg had little effect upon the failure times. All failure times for the case with normal friction factors mirror the results of the conventional test.

4.0 FINDINGS

An analysis was performed to evaluate the capability of RELAP5/MOD3 to calculate hot leg natural circulation phenomena in a PWR. Data on natural circulation came from a battery of tests performed at the Westinghouse Research and Development Center, where a 1/7 scale PWR model was constructed. The Westinghouse tests were performed using three different fluids, but the high pressure tests using SF_6 as the working fluid were the ones which this analysis aimed at simulating.

Several assumptions were made in the construction of the RELAP5/MOD3 input in order to model the Westinghouse experiments, particularly within the hot leg geometry. First, the Westinghouse personnel reported a sloped countercurrent flow interface in the hot leg. To simulate this, the model contained two sloped pipes for the hot leg, a revision over the split hot leg used in previous RELAP5/MOD3 analyses. Each pipe represented one flow direction of the countercurrent flow. Second, the inlet plenum of the steam generator was subdivided into three volumes according to the mixing factor, $F_{\blacksquare}$, which was reported by Westinghouse. And finally, the friction coefficient in the hot leg accounted for the higher drag along the hot/cold countercurrent interface.

Using the model built under these assumptions, computational runs were performed until the conditions in the hot leg matched closely with the conditions reported by Westinghouse to exist in the hot legs of their experimental apparatus. In this way, when the conditions did match, all of the assumptions built into the model could be justified in terms of the Westinghouse results. The obvious conclusion to be drawn after the conditions matched is that RELAP5/MOD3 is able to calculate hot leg countercurrent flow natural circulation phenomena, at least in this geometry. It is likely, however, that other geometries exist which would also be able to match the Westinghouse data, given the right

initial conditions. But this analysis only set out to prove that there existed one geometry capable of duplicating the Westinghouse test results.

The purpose of this research was to verify the ability of RELAP5/MOD3 to predict natural circulation phenomena and compare it against experimental data. For the geometry used, RELAP5/MOD3 worked very well. However, it should be pointed out that the geometry which was used in this case is not exclusive to these results. Conceivably, there are multiple geometries which would work as well as, if not better than, the geometry which was used in this case. However, it is encouraging that RELAP5/MOD3 worked so well in a geometry wholly dictated and justified by the experimental results compiled by Westinghouse.

It is further noted that the particular geometrical constants whose values were varied until convergence with experimental results was attained, though they are the preferred constants, are not the only constants which could have been varied. Similar results could have been achieved by drastically altering the amount of heat removed by structures in the model, by decreasing the size of particular volumes while at the same time increasing the k_{loss} coefficient, or by otherwise affecting the pressure head which was artificially established in the hot legs.

Once the Westinghouse test results were duplicated on the scale of the experimental apparatus, the geometry of the final small scale model was applied to a full-size PWR, the Surry plant model. Three cases were run with the Surry model. First, the normal split hot leg was run as a control run. Second, the revised split hot leg was applied with an enhanced friction factor to the full-size model. And third, the revised split hot leg was applied to the full-size model, but the friction factor in the hot leg was not changed to reflect the increased friction from the countercurrent flow interface.

The results indicate that the slope modeled in the revised split hot leg has little, if any, effect upon the duration and end result of the transient. While failure time is accelerated slightly, the time to failure is essentially the same for all cases. However, in the case of the revised split hot leg with the enhanced friction factor, the lower head failure occurs nearly ten minutes after the failure of the lower head in the other runs. This is accounted for by the fact that greater heat transfer occurs between the core and the upper internals, including the hot leg, due to higher friction in an enhanced natural circulation system.

Overall, though, it appears that RELAP5/MOD3 is able to account for single-phase heat transfer due to natural circulation between the core and the internals of the RPV, as well as with the hot leg, as long as the geometry is initialized correctly. For example, the split hot leg is necessary, due to the one-dimensional ability of the code, in order to give the fluid two directions in which to flow. The code would be unable to calculate a countercurrent flow pattern if a single pipe were to be used as the model for the hot leg.

There are several different areas which would be beneficial to examine further. First, a calculation could be done to determine a heat transfer coefficient between the superheated fluid in the hot leg and the walls of the pressurizer surge line. Second, a similar calculation could be made between the superheated vapor in the steam generator inlet plenum and the steam generator tubing. Both of these calculations would be beneficial because they would allow investigators to make simple calculations of the time to heat up and failure of these parts during similar transients. Further investigation into the ability of thermal hydraulic codes to handle natural circulation phenomena in other types of plants would also be beneficial, in particular if the events at Three Mile Island could be effectively duplicated through the use of a code.

The importance of this exercise is that the results establish a good relationship between the results of an experimental investigation

and a computer simulation of the same situation. An increasing degree of confidence is thus lent to calculational results and suppositions which previously have had limited benchmarking.

5.0 REFERENCES

1. W. A. Stewart, A. T. Pieczynski, and V. Srinivas, *Experiments on Natural Circulation in a Pressurized Water Reactor Model for Degraded Core Accidents*, EPRI Project No. RP2177-5, Final Report.

2. W. A. Stewart, A. T. Pieczynski, and V. Srinivas, *Experiments on Natural Circulation in a Pressurized Water Reactor Model with High Pressure SF_6*, Preliminary Draft.

3. S. V. Chmielewski, *Calculation Package: RELAP5/MOD3 Input Preparation for Westinghouse 1/7 Scale Model Using High Pressure SF_6*, October, 1991.

4. P. D. Bayless, *Analyses of Natural Circulation During a Surry Station Blackout Using SCDAP/RELAP5*, NUREG/CR-5214, EGG-2547, October, 1988.

5. W. A. Stewart, A. T. Pieczynski, and V. Srinivas, "Experiments on Natural Circulation Flows in Steam Generators During Severe Accidents, *Proceedings of the International ANS/ENS Topical Meeting on Thermal Reactor Safety*, San Diego, CA, February 2-6, 1986.

6. Letter, S. V. Chmielewski to R. J. Wagner, "SF_6 Properties," SVC-2-91, August 13, 1991.

APPENDIX A

This appendix contains an excerpt from the calculation package which developed the model for the Westinghouse 1/7 scale experimental apparatus. In particular, this appendix contains the methodology for developing the revised (sloped) split hot leg.

2.5 Hot Legs

There are two hot legs attached to the pressure vessel in the experimental apparatus. Thus, two hot legs will be modeled, a left-side hot leg and a right side hot leg. Dimensions for the hot leg are derived from the assembly drawing, Ref. 6. No pressurizer will be modeled, for the experiments were performed without one.

Within the hot leg, the fluid is stratified into a hot flow and a cold countercurrent flow. The interface between this stratified flow slopes upward towards the steam generator end. This induces a vertical pressure gradient towards the steam generator for the hot flow, and towards the pressure vessel for the cold flow, hence countercurrent flow. The pressure gradient provides the force necessary to overcome wall and interface effects and cause flow to move. The interface boundary is sloped due to the shear stresses encountered on the counterflow interface. Therefore, the sloped interface provides the pressure forces for flow, which in turn leads to interface shear stress, causing a sloped interface.

Because this deck is to be used in particular to model stratified countercurrent flow in the hot legs, some attention should be given to detailing the model to provide sufficient pressure driven flow through the hot legs. Additionally, this deck will strive to duplicate certain results from the Westinghouse data. Thus, the hot leg geometry with respect to a hot/cold fluid interface will be artificially sloped such that countercurrent flow will be induced by the pressure differential, thus simulating buoyancy driven flow.

In real countercurrent flow in the hot leg, the pump loop seals are blocked off by liquid water, which removes the cold leg from the flow path. Consequently, fluid in the hot leg flows in both directions. In order to model this phenomenon, the hot leg will be divided in half and modeled by two pipe components. Also, the slope of the hot/cold fluid interface will be artificially set in order to induce the correct flow

pattern.

The two hot legs are identical to each other. The input which follows will describe only the right-side hot loop, but will also apply to the left-side hot loop.

To begin with, it is necessary to choose a slope for the hot/cold interface in the hot leg. My assumption will be a sloping 65/35 division at each end of the hot leg. In the Westinghouse tests, they measured a 73/27 slope division at each end of the hot leg. In this case, this means that at the intersection of the hot leg with the pressure vessel, 65% of the flow is in the hot part of the hot leg, while 35% of the flow is in the cold part of the hot leg. Conversely, at the steam generator inlet plenum, 35% of the flow is in the hot part of the hot leg, while 65% of the flow is in the cold part of the hot leg.

The hot leg itself is divided into four sub-components along its length. The lengths of these sub-components is shown in the following table:

Volume Number	Length (ft)
185-01/180-04/285-01/280-04	.3542
185-02/180-03/285-02/280-03	.6825
185-03/180-02/285-03/280-02	.6825
185-04/285-04	.1974
180-01/280-01	.354167

Since the walls of pipes which represent the hot legs cannot themselves have a slope, the flow areas of each individual sub-volume in the hot part of the hot leg will have a smaller flow area than the one

immediately preceding it in the flow path, such that a line drawn through the midpoints of each sub-volume in the hot part of the hot legs has the desired slope of the hot/cold interface, as shown in Figure 4.

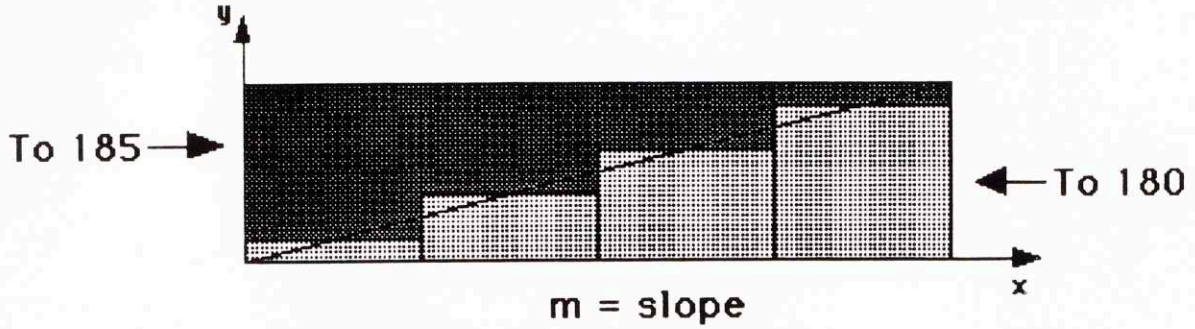

. Hot Leg Hot/Cold Interface and Slope.

In the hot part of the hot leg, each flow area of each volume will be represented by a percentage of the total flow area of the pipe. Total flow area of the pipe is πR^2, or 8.84046e-2 ft^2. Total length of the hot part of the hot leg is 1.97625 ft. The slope of the hot/cold interface, therefore, is:

$$slope = m = \frac{.35-.65}{1.97625} = -1.518e-1$$

Using this slope, values for the percentage of flow area can be found to be the following:

x (ft)	y (%)
0.0	.65
.3542	.59623
1.0367	.49263
1.7192	.389021

1.97625 .35

These values represent the percentage of flow area at the endpoints of each volume for a perfectly represented hot/cold interface. To get the approximate values of the flow area for each volume, average the values of the endpoints for the four volumes:

% volume 1 (185-01) = (.65 + .59623)/2 = .62312

% volume 2 (185-02) = (.59623 + .49263)/2 = .54443

% volume 3 (185-03) = (.49263 + .389021)/2 = .44082

% volume 4 (185-04) = (.389021 + .35)/2 = .36951

The hot/cold interface will be represented as a perfect chord of length l which divides the pipe into two areas, as shown in Fig. 5.

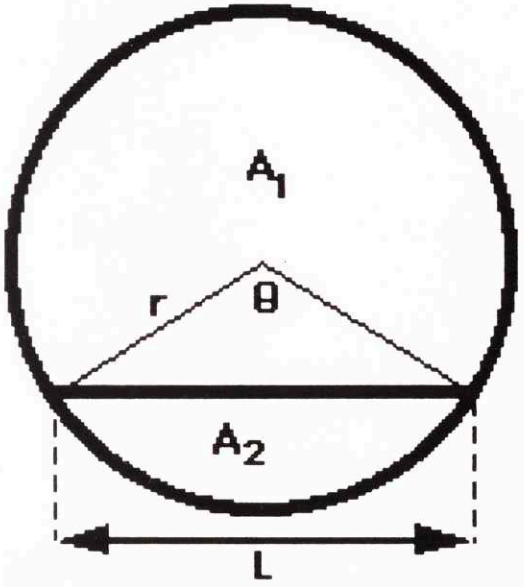

. Hot Leg Hot/Cold Interface Within the Pipe.

The appropriate equations are as follows:

$$A_2 = \frac{r^2}{2}(\theta - \sin\theta)$$

$$l = 2r \sin(\frac{\theta}{2})$$

In this case, r is the radius of the pipe, 1.6775e-1 ft. P_w is the wetted perimeter, calculated by :

$$P_w = r\theta + l$$

Using the above equations, the following information can be calculated.

volume #	A_2 (ft^2)	θ (rad)	l (ft)	P_w (ft)
1	5.5087e-2	3.5334	3.2908e-1	9.2181e-1
2	4.8130e-2	3.2814	3.3468e-1	8.8514e-1
3	3.8971e-2	2.9551	3.3404e-1	8.2976e-1
4	3.2666e-2	2.7257	3.2827e-1	7.8551e-1

The value of A_2 is the flow area of that particular volume. It is necessary to calculate a surface roughness factor and the hydraulic diameter. The countercurrent flow interface will be assumed to be a very rough pipe, f = 0.07, ϵ = ~.03. The value of ϵ for the hot leg pipe itself is 1.5e-4. The surface roughness factor will be a perimeter averaged value. To be calculated accurately, the percentage of flow perimeter which is countercurrent flow interface must be calculated. This percentage is simply $1/P_w$.

volume #	% P_w	$\overline{\epsilon}$	D_h
1	.4179	6.312e-3	2.3904e-1
2	.3781	5.718e-3	2.1750e-1
3	.40257	6.083e-3	1.8782e-1
4	.4179	6.312e-3	1.6634e-1

Components 200, 201, and 202 (300, 301, and 302) describe the inlet plenum to the steam generator. The inlet plenum is divided into a hot region (components 200,300), a mixing region (components 201,301), and a cold region (components 202,302).

As described in Ref. 5, the inlet plenum is a 20.00" OD, 19.00" ID, half-hemisphere, which has a divider plate 0.5" thick in it. The inlet plenum, also called the channel heads, center point is 1.62" below the bottom of the tubesheet. Thus, the volume of the inlet plenum is one-fourth the volume of the sphere, minus 1/2 the volume of the divider plate, plus the area 1.62" above the half-hemisphere. This area is semi-circular, so it can be calculated as follows:

$$V_+ = \pi * \frac{1}{2} ** (\frac{19.00}{2})^2 * 1.62 = 229.660\ inches^3 = .132905\ ft^3$$

The volume of the rest of the inlet plenum is as follows:

$$V_{1/4\ hemisphere} = \frac{1}{4} * \frac{4}{3} * \pi * \left(\frac{ID}{2}\right)^3 = .519585\ ft^3$$

The volume of the divider plate is:

$$V_{d.p.} = \frac{1}{2} * \pi * \left(\frac{ID}{2}\right)^2 * t + \frac{1}{2} * 1.62'' * 19.00'' * t = 4.10198e\text{-}2 + 4.453e\text{-}3$$

Thus, the volume of the inlet plenum is:

$$V_{Inlet\ Plenum} = V_{\frac{1}{2}hemisphere} + V_{+} - V_{d.p.} = .519585 + .132905 - .045472$$

From test SG-S2, data included as Ref. 7, the mixing fraction in the inlet plenum is 0.89. Thus, 89% of the volume in the inlet plenum is involved in mixing, or is in component 201/301, and the remaining 11% is split equally between components 200 (300) and 202 (302). The volumes are as follows:

Component 201 = $.89 * V_{inlet\ plenum} = .540246\ ft^3$

Component 200 = $0.5 * (1-.89) * V_{inlet\ plenum} = 3.3386e\text{-}2\ ft^3$

Component 202 = Component 200 = $3.3386e\text{-}2\ ft^3$

In the inlet plenum, components 200 and 201 (300 and 301) are connected via junctions to the hot part of the hot leg, component 185 (285). The individual junction flow areas need to be specified, or else the code takes the minimum volume of the two connecting volumes as the flow area. In this case, that would constitute too much flow area. Recall that the mixing fraction, f, is 0.89. Thus, 89% of the flow area of volume 4 of component 185 (285) connects to the mixing volume, component 201 (301), and the other 11% connects to the hot volume of the inlet plenum, component 200 (300).

In the same way, the return flow from the inlet plenum to volume 1 of component 180 (280), the cold hot leg flow, is through components 201 and 202 (301 and 302). Again, 89% of the flow area in component 180 (280) connects the mixing volume 201 (301) to the return flow, and 11% of the flow area in component 180 (280) connects the cold volume 202 (302) to the return flow.

Additionally, the inlet plenum junctions to the steam generator tubes are handled in a similar fashion. As will be developed below, 35% of the SG tubes support hot fluid flow, while the remaining 65% support cold fluid flow. Therefore, for the junction between the hot inlet plenum volume and the hot tubes, the flow area is 11% of the 35% of the total flow area of the hot SG tubes. Similarly, 89% of the 35% of the hot SG tubes are junctioned with the mixing inlet plenum volume. The same method is used for the cold SG tube flow and the mixing and cold volumes in the inlet plenum. The flow areas for the SG tubes are listed below.

Components 203 (303) and 204 (304) represent steam generator u-tubes. As with the hot leg countercurrent flow exit into the inlet plenum, 65% of the steam generator tubes will flow with cold fluid, and the remaining 35% will flow with hot fluid. Ref. 5 contains information on the steam generator tubes, and Ref. 8 identifies individual row lengths of steam generator tubes.

There are 216 total tubes, OD of .375", ID of .305". This makes the total flow area from the inlet plenum to be:

$$A_{total,tubes} = 216 * \pi * (\frac{ID}{2})^2 = 15.78132\ inches^2 = .10959\ ft^2$$

Then, the area for the hot tubes and the cold tubes is, respectively:

$$A_{hot,tubes} = .35 * A_{total,tubes} = 3.8357e\text{-}2\ ft^2$$

$$A_{cold,tubes} = .65 * A_{total,tubes} = 7.1235e\text{-}2\ ft^2$$

Recall that the mixing factor, f, for the steam generator inlet plenum is **0.89**. In order that the proper flow be modeled, the junction areas between inlet plenum volumes and steam generator tube volumes must be specified. Thus, 89% of the inlet flow area to component 203 (303) must connect to the mixing volume in the inlet plenum, component 201 (301). By the same reasoning, 89% of the flow area from component 204 (304), the cold steam generator tubes, should connect to the mixing volume, component 201 (301). The remaining 11% of the flow area to the hot tubes should flow from the hot inlet plenum volume, component 200 (300), and the remaining 11% of the cold hot tube junction area should flow to the cold inlet plenum volume, component 202 (302). Therefore:

$$A_{hot,mixing} = 0.89 * A_{hot,tubes} = 3.4138e\text{-}2\ ft^2$$

$$A_{hot,hot} = A_{hot,tubes} - A_{hot,mixing} = 4.2193e\text{-}3\ ft^2$$

$$A_{cold,mixing} = .89 * A_{cold,tubes} = 6.3399e\text{-}2\ ft^2$$

$$A_{cold,cold} = A_{cold,tubes} - A_{cold,mixing} = 7.8359e\text{-}3\ ft^2$$

Next, the steam generator tube geometry must be calculated for input. From Ref. 8, the following information can be derived:

- U-bend starts 42.93" above tubesheet
- Length of straight section = 2 * 42.93" = 85.86"
- Top of highest U-bend = 51.56"
- Top of lowest U-bend = 43.82"

- Average Radius of U-bend = 3.994"
- Average centerline elevation = 46.926"
- Average tube length = 107.406"
- Thickness of support plate = 4.5"

The height of the average tube, then, is the thickness of the support plate plus the average radius of the U-bend plus one-half of the length of the straight section:

$$Avg\ height\ of\ u\text{-}tube = \tfrac{1}{2}*85.86 + 4.5 + 3.994 = 51.424\ inches$$

The steam generator tubes will be divided into 4 sections along its height, or 8 sections total (8 sub-volumes). Thus, the height of each section is one-fourth the height of the average tube, or 12.856".

However, the top two sub-volumes, sections 4 and 5, contain the U-tube bend. While the individual height of these volumes is 12.856", the total flow length of section 4 is equal to the individual height of this section plus half of the average tube length minus the average height of the tubes, or:

$$flow\ length = 12.856 + \tfrac{1}{2}*107.406 - 51.424 = 15.135\ inches = 1$$

The inclination angle, then, for section 4 is calculated as follows:

$$\arcsin\left(\frac{12.856}{15.135}\right) = 58.15°$$

Components which represent steam generator tubes will be pipe components.

Next, the exit plenum of the steam generator needs to be modeled. Component 205 (305) represents the exit plenum of the steam generator. The total volume of the exit plenum is equal to the total volume of the inlet plenum, $V_{Inlet\ Plenum}$, calculated above. Component 205 is a branch component.

The final component of the hot leg is the cold return flow to the RPV, or the cold part of the hot/cold interface in the hot leg. This is represented by a pipe for component 180 (280). A calculation scheme similar to that done for component 185 must be performed. However, it is important to note that the first volume of component 180 is longer than its corresponding volume in component 185, which is the fourth volume. Thus, the slope of the cold/hot interface must be recalculated in order to get the correct flow area percentages, P_w, and average roughness.

In the cold part of the hot leg, each flow area of each volume will be represented by a percentage of the total flow area of the pipe. Total flow area of the pipe is πR^2, or 8.84046e-2 ft^2. Total length of the cold part of the hot leg is 2.03587 ft. The slope of the hot/cold interface, therefore, is:

$$slope = m = \frac{.65-.35}{2.03587} = 1.474e-1$$

Using this slope, values for the percentage of flow area can be found to be the following (where x = 0.0 is the point where the hot leg joins to the RPV):

x (ft)	y (%)
0.0	.35
.31670	.39667

.9992	.49724
1.68170	.59781
2.03587	.65

These values represent the percentage of flow area at the endpoints of each volume for a perfectly represented hot/cold interface. To get the approximate values of the flow area for each volume, average the values of the endpoints for the four volumes:

% volume 1 (180-01) = (.65 + .59781)/2 = .62390

% volume 2 (180-02) = (.59781 + .49724)/2 = .54752

% volume 3 (180-03) = (.49724 + .39667)/2 = .44696

% volume 4 (180-04) = (.39667 + .35)/2 = .37334

Using the equations used for component 185 above, the following information can be calculated.

volume #	A_2 (ft^2)	θ (rad)	l (ft)	P_w (ft)
1	5.5156e-2	3.5359	3.2900e-1	9.2215e-1
2	4.8404e-2	3.2912	3.3456e-1	8.8665e-1
3	3.9513e-2	2.9746	3.3433e-1	8.3331e-1
4	3.3004e-2	2.7382	3.2870e-1	7.8804e-1

The value of A_2 is the flow area of that particular volume. It is necessary to calculate a surface roughness factor and the hydraulic diameter. The countercurrent flow interface will be assumed to be a very rough pipe, $f = 0.07$, $\epsilon = \sim.03$. The value of ϵ for the hot leg

pipe itself is 1.5e-4. The surface roughness factor will be a perimeter averaged value. To be calculated accurately, the percentage of flow perimeter which is countercurrent flow interface must be calculated. This percentage is simply $1/P_w$.

volume #	% P_w	$\overline{\epsilon}$	D_h
1	.3568	5.40e-3	2.3925e-1
2	.3773	5.71e-3	2.1837e-1
3	.4012	6.06e-3	1.8967e-1
4	.4171	6.30e-3	1.6753e-1